Time-resolved ultraviolet spectroscopy of the compact interacting binary QU Car*

L. E. Hartley[1], J. E. Drew[1], K. S. Long[2]

[1] *Astrophysics Group, Department of Physics, Imperial College, Prince Consort Road, London SW7 2BW*
[2] *Space Telescope Science Institute, 3700 San Martin Drive, Baltimore, MD 21218*

20 December 2007

arXiv:astro-ph/0207030v1 1 Jul 2002

ABSTRACT

We present *HST*/STIS (1160–1700 Å) echelle spectra of the cataclysmic variable (CV) star, QU Car, at three epochs. In catalogues this binary is classified as a nova-like variable. QU Car was observed three times in time-tag mode for 2300 sec, 2600 sec and 2600 sec, allowing us to study the spectral time evolution on timescales down to ∼10 sec. We find evidence of a high-state non-magnetic CV at low inclination, with unusually high ionisation.

We observed narrow absorption lines ($\sim$ few hundred km s^{-1} wide) in N V λ 1240, O V λ 1371 and Si IV λ 1398, as well as broader (HWZI $\sim$ 1000 km s^{-1}) emission in C III λ 1176, C IV λ 1549 and He II λ 1640, all with a superposed absorption component. High ionisation is indicated by the He II emission, which is unusually strong in comparison with C IV, and the relative strength of the O V absorption line. The dereddened UV continuum spectral index of, on average, −2.3 suggests that disc accretion dominates the spectral energy distribution. In two observations velocity shifting is noted in the absorption lines on a timescale long enough not to repeat within the ∼ 2600-sec exposures. The absorption superposed on the C IV emission line moves coherently with the N V and Si IV absorption, suggesting the same origin for all absorption lines – most likely to be in the accretion disc atmosphere.

Weak blueshifted absorption in N V and C IV provides evidence of an outflow component and we estimate a maximum outflow velocity of $\sim$ 2000 km s^{-1} . This may be linked to a wind launched from further out in the disc than is typically seen in those high-state non-magnetic CV whose wind speeds are observed to reach to $\gtrsim$ 4000 km s^{-1} . Unusually, three ionisation stages of carbon – C II, C III and C IV – are present in emission, with line width increasing with higher ionisation. The presence of C II in emission and the positive line-width/ionisation correlation is most easily reconciled with an origin in a disc chromosphere, beyond the influence of the EUV-emitting inner disc.

Key words: binaries: close – stars: mass-loss – novae, cataclysmic variables – ultraviolet: stars – line: profiles – stars: individual: QU Carinae

1   INTRODUCTION

Cataclysmic Variable (CV) stars are interacting binary systems in which a late-type secondary star overflows its Roche lobe and accretes matter onto a compact primary. Amongst these, the nova-like variables are defined as those that persist in a high mass-accretion rate. A result of such a heterogeneous label is that, amongst the nova-like variables, there are many objects that, displaying similarities to members of other CV classes, sit uneasily with their classification. In

this paper we present high time-resolution UV spectroscopy of one such example – QU Car.

At $m_{\rm v}$ = 11.4, QU Car is one of the brightest known CV, so it is rather surprising that until now it has been mostly ignored in observational studies. From among the small number of hitherto published studies, Gilliland & Phillips (1982) examined optical spectra (4300–4800 Å) at time-resolutions down to 3 minutes. They derived a long period (10$^{\rm h}$9) from radial velocity variations in the optical

emission lines. They also made note of the relative weakness of the Balmer line emission, which they deemed due to a high temperature and high mass accretion rate in the disc and suggested a classification of old nova or nova-like variable – a view in keeping with Schild's (1969) comment that the object displayed some characteristics indicative of an old nova. Since this time, QU Car has been classified in catalogues (Ritter & Kolb 1998, Downes et al. 2001) as a nova-like variable.

International Ultraviolet Explorer (*IUE*) low-dispersion spectra reveal broad blueshifted UV absorption lines in N V and C IV, with an emission component in C IV and He II (Knigge, Woods & Drew 1994), indicative of an optically thick disc accompanied by mass outflow. Knigge et al. (1994) noted variation in the C IV line caused by a periodic increase in the strength of the emission component, but were unable to decide whether this variablity was linked to the orbital phase. They also commented on the strength of the O V λ 1371 absorption line and the He II λ 1640 emission – both unusually strong for high-state non-magnetic CV (Hn-MCV).

The data that are analysed in this paper were obtained as part of an observing campaign to detect spectral signatures of disc-wind variability of short timescales. These signatures are predicted to show up as highly time-variable fine structure components in wind-formed UV lines (Proga, Stone & Drew 1998). To achieve the necessary time and wavelenght resolution, the Space Telescope Imaging Spectrograph (STIS) on the *Hubble Space Telescope* (*HST*) was employed with an echelle grating in photon-counting (TIME-TAG) mode. This allows a time-resolution of down to $\sim 10\,\mathrm{s}$ and velocity resolution of down to $\sim 10\,\mathrm{km\,s^{-1}}$, with the trade-off that higher time-resolution will result in a reduced useable spectral resolution and vice-versa.

On examining the results of the *HST* observations we were struck by the ways in which QU Car distinguished itself from the other targets in the programme (the nova-like variables IX Vel and V3885 Sgr, presented in Hartley et al. 2002). In this paper we seek to present the current *HST* observations and then re-examine archive data, with a view to establishing a physical origin for the unusual features noted. In section 2 we describe the observations and data extraction processes. The results are then presented in two ways: in section 3 we describe the time-averaged spectrum obtained at each epoch of observation, then in section 4 we re-present the data as spectral time-series at 30-sec time-resolution and as continuum light curves. Finally, in section 6 we complare QU Car with other non-magnetic HnMCV and consider the origin of QU Car's UV line spectrum.

2 OBSERVATIONS AND DATA EXTRACTION

Observations were performed by the STIS instrument on the *HST* with the far ultraviolet (FUV) MAMA detector (1140–1735 Å). The E140M echelle grating with a central wavelength of 1425 Å was used. This configuration provides a resolution of $\sim 13\,\mathrm{km\,s^{-1}}$ (R $\sim$ 23000). Each observation was performed in a single telescope orbit for the maximum available time, with the detector set to time-tag mode and using the $0.2''\times0.2''$ aperture. The dates and exposure lengths of our observations are given in table 2.

Observation date (2000)	Label	U.T. start time	Exposure (s)
12th Feb	Q1	20:26:07	2300
24th July	Q2	07:13:34	2600
16th Sep	Q3	02:56:32	2600

Table 1. The observation dates and times for each observing run

All data calibration was performed with IRAF software, using the STSDAS package produced by the Space Telescope Science Institute (STScI). Time-tag is a photon counting mode, which provides an events stream with 125-μs time-resolution. This can be integrated over any selected time resolution (time bin) to produce a set of raw images of the echelle output, from which a 1-D spectrum is extracted and calibrated. The calibration, including doppler correction for the telescope's motion, was performed with STScI's CALSTIS package, using the suggested best reference files.

3 THE MEAN UV SPECTRUM

figure 1 shows the summed spectrum for each observation (hereafter called datasets Q1, Q2 and Q3). QU Car's UV lines appear to be characterised by strong absorption features in N V λ 1240 and O V λ 1371, less prominent Si IV λ 1398 absorption, and emission in C III λ 1176, C IV λ 1549 and He II λ 1640. The narrowness of QU Car's line features is striking. Typical terminal velocities of outflows in high-state CV that commonly determine UV line widths can be up to $5000\,\mathrm{km\,s^{-1}}$. Indeed it is usual to find broad blueshifted absorption in the stronger resonance line profiles in non-eclipsing systems. Here, however, the line profiles rarely extend to more than $\sim \pm1000\,\mathrm{km\,s^{-1}}$, and show rather little P Cygni behaviour.

The STIS datasets offer an insight into the finer structure of lines that have previously only been identifiable in *IUE* low-resolution data. However, before describing the character of the observed profiles, we first consider whether it is possible to correct the spectra for line of sight (LOS) motion of the white dwarf (WD). Gilliland & Phillips (1982) calculated a spectroscopic zero-phase ephemeris of $T_0 = 2443960.683 \pm 0.003\,\mathrm{JD}$ and a period of $10^{\mathrm{h}}.896 \pm 0.336$ from velocity shifts in the He II λ 4686 emission line. However, the uncertainty in the phase measurement is such that we are unable to determine the orbital phase of the data presented here. So no radial velocity correction can yet be applied to the spectral lines. Nevertheless, the orbital K-velocity ($K_{\mathrm{WD}} = 115 \pm 13\,\mathrm{km\,s^{-1}}$) and radial velocity ($\gamma = -84 \pm 20\,\mathrm{km\,s^{-1}}$) derived by Gilliland & Phillips suggest the data are radial velocity shifted from the WD rest frame by no more than $\sim 200\,\mathrm{km\,s^{-1}}$ bluewards and $\sim 30\,\mathrm{km\,s^{-1}}$ redwards.

Figure 2 presents time-averaged close-ups of the strongest lines apparent in QU Car's UV spectrum, at each epoch of observation, with the wavelength given in the heliocentric frame.

N V λ λ 1238.8, 1242.8 doublet is the transition that shows the most secular variation. In Q1 the gross structure of the N V profile bears the mark of an outflow component with a broad asymmetric absoption trough that stretches
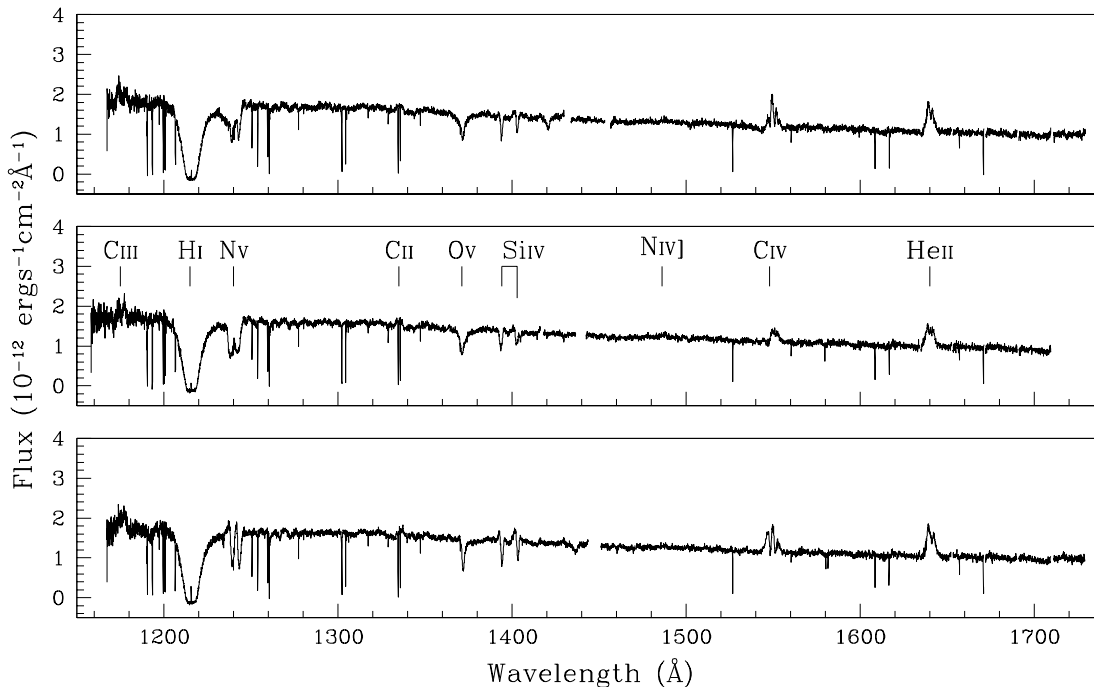
Figure 1. The summed spectrum for (from top to bottom) 12th January, 21st July and 16th September 2000. Resonance transitions and other strong lines are indicated.

from approximately -2000 to $+1500 \, \mathrm{km \, s^{-1}}$, relative to the bluemost component of the doublet ($+500 \, \mathrm{km \, s^{-1}}$ relative to the red component). Superposed on this broad structure are narrower absorption troughs, $\sim 400 \, \mathrm{km \, s^{-1}}$ FWHM, centred on the doublet rest wavelengths. In Q2 the N v λ 1240 line is in absorption from -600 to $\sim +1500 \, \mathrm{km \, s^{-1}}$, with each component of the doublet clearly defined, but overlapping slightly and more rounded than in the other sets. In Q3 there is clearly blueshifted emission in N v (to no more than $-1000 \, \mathrm{km \, s^{-1}}$) and the absorption minumum is redward of heliocentric rest at about $+100 \, \mathrm{km \, s^{-1}}$. Without knowing the exact LOS velocity correction we cannot be certain that the absorption minimum is redshifted in the primary frame - such a conclusion rests heavily on the adopted *gamma* velocity. If the maximum likely white-dwarf (primary) redshift really is no greater than $\sim 30 \, \mathrm{km \, s^{-1}}$ (see above), the absorption minimum remains at net redshift.

During the first epoch of observation, Q1, the O v line is broad with absorption reaching to at least $\pm 1500 \, \mathrm{km \, s^{-1}}$. The profile shows a skew that suggests stronger absorption in the blue wing, indicating some contribution from an outflow. This transition is remarkably strong compared to other nova-like variables in which it is seen as a weak, rotationally-broadened, disc-formed line, if seen at all (c.f. the HST/STIS data on IX Vel and V3885 Sgr presented in Hartley et al 2002)). In all three datasets the Si iv λ 1398 absorption profile, seen in both doublet components, is about $250 \, \mathrm{km \, s^{-1}}$ wide (FWHM). There is no blueshifted absorption at any time analogous to that seen in N v and weakly in O v.

The changes seen in Si iv λ 1398 and O v λ 1371 are similar, but less marked than those seen in the N v line – this lends a general pattern to QU Car's core line absorption: In

Q1 we see fairly symmetrical, almost triangular absorption; in Q2 the lines are somewhat more rounded; in Q3 there is a definite redwards skew to the absorption lines, with blueshifted emission components obvious in N v and Si iv.

The C iii λ 1176, C iv λ 1549 and He ii λ 1640 lines are in emission to about $\pm 1000 \, \mathrm{km \, s^{-1}}$. The C iv and He ii emission lines are respectively triple- and double-peaked with peak separations of $\sim 400 \, \mathrm{km \, s^{-1}}$. Significantly, the absorption minima in C iv are separated by the intrinsic doublet splitting of $484 \, \mathrm{km \, s^{-1}}$ (to within measurement errors). In all observations the C iii line's emission peaks are split by $800 \, \mathrm{km \, s^{-1}}$ – the individual components of this six-component transition span $370 \, \mathrm{km \, s^{-1}}$. The most plausible interpretation of the profile morphology is that, in each case, a broad (FWHM $\sim 1000 \, \mathrm{km \, s^{-1}}$) emission feature is cut into by narrower absorption, broadened kinematically to only FWHM $\sim 400 \, \mathrm{km \, s^{-1}}$. The shapes of the absorption components resemble the shapes of the absorption-dominated N v , O v and Si iv lines discussed above. The physical origin of the line spectrum will be considered later in section 6.

We note little secular variation in the emission lines, although, Q2 does set itself apart from the other two observations. Firstly, the emission lines are weaker than in the other datasets, whilst there is not much corresponding weakening of the superposed absorption components. Also, in Q2, the C iv line has lost its triple-peaked shape, becoming instead what appears as a weak P Cygni form with redshifted emission from -200 to $+1400 \, \mathrm{km \, s^{-1}}$ and a hint of blueshifted absorption also.

Before making a fit to the spectral energy distribution, the spectrum was dereddened using $E(B - V) = 0.1$ given in Verbunt (1987). A power law continuum fit was made to
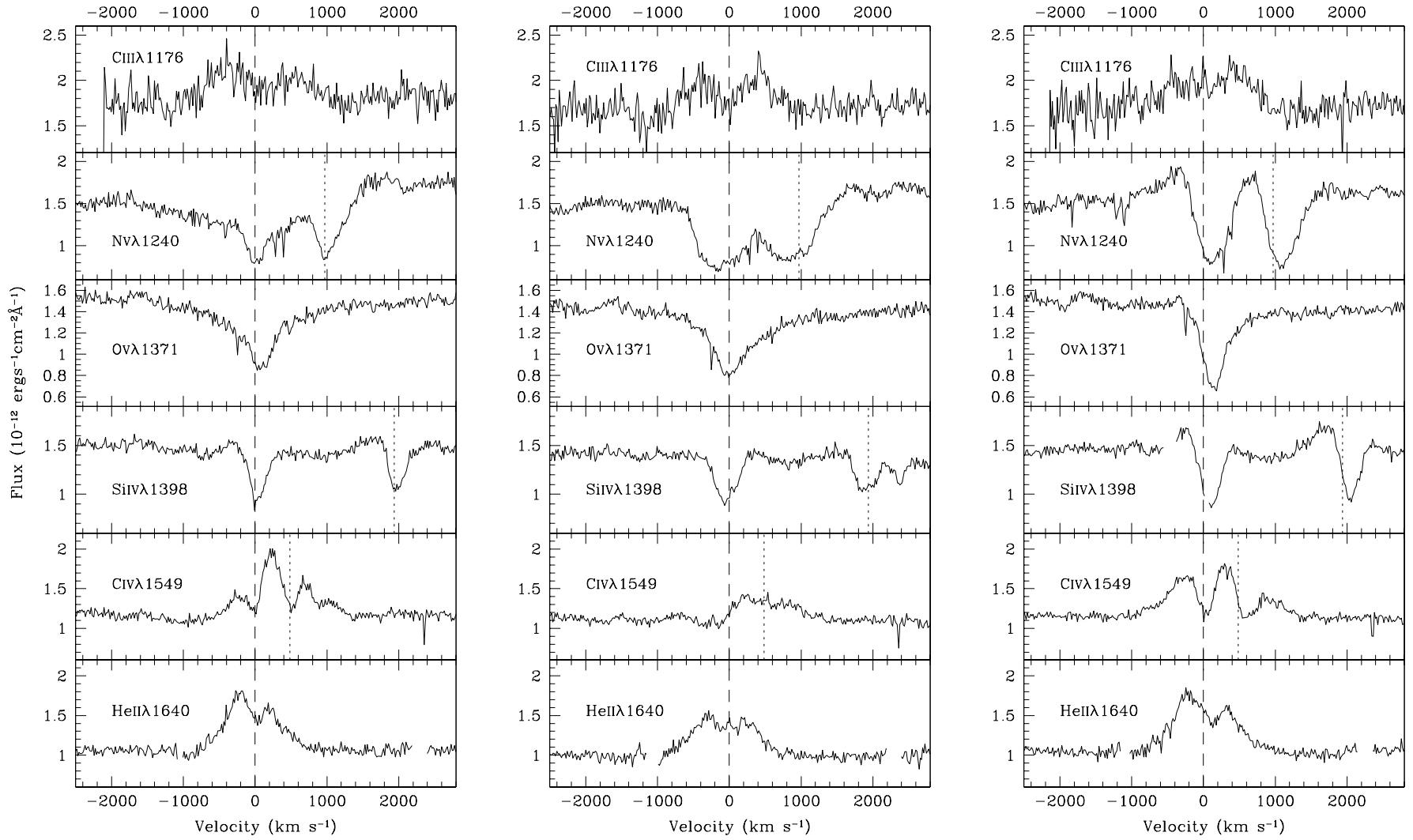
Figure 2. Time-averaged C III λ 1175, N v λ 1240, O v λ 1371, Si IV λ 1398, C IV λ 1549 and He II λ 1640 lines for, from left to right, Q1, Q2 and Q3. In doublet lines velocity shifts are measured with respect to the bluemost component, shown by the dashed vertical line. The longer wavelength component is marked by a dotted vertical line. Note that the flux scale is selected arbitrarily to show most clearly the line profile structure and in some cases the zero is supressed.

Table 2. Mean continuum flux level in the range 1270–1320 Å, with mean continuum flux and index of power law continuum fit, when the spectrum is dereddened with $E(B-V) = 0.1$. Flux units are $\times 10^{-12}\,\mathrm{erg\,s^{-1}\,cm^{-2}\,Å^{-1}}$. Error is one standard deviation from the mean.

Label	Flux	Dereddened Flux	Index
Q1	1.66 ± 0.13	3.88 ± 0.12	-2.32 ± 0.05
Q2	1.56 ± 0.13	3.65 ± 0.13	-2.45 ± 0.10
Q3	1.61 ± 0.13	3.75 ± 0.10	-2.24 ± 0.08

the mean spectrum, after masking out areas obviously contaminated by spectral lines. Table 2 lists the spectral index measured from each mean spectrum and the average flux level in the 1260–1270 Å range. We note very little variation in the continuum flux from observation to observation. QU Car's spectral index over the ~ 500 Å available to us is -2.4 on average, fitting in well with other nova-like variables, for example IX Vel (-2.4) and V3885 Sgr (-2.3) (Hartley et al. 2002). Corrected for the same assumed reddening, merged short and long wavelength IUE spectra of QU Car spanning nearly 2000 Å fit to a power law index of -2.25 ± 0.1 (see Drew et al. 2002). This suggests the UV spectral energy distribution is reasonably stable over time.

4   VARIATION ON TIMESCALES SHORTER THAN $\sim$ 2500 SEC

An analysis of time-variability of the strong lines during each observation is presented in this section. The N V λ 1240, O V λ 1371, Si IV λ 1398 and C IV λ 1549 lines are displayed as trailed mean-subtracted spectra, as trailed normalized spectra and as 1D averages of the first and the second half of the 2600-sec observation. In the trailed spectra we include only observations Q2 and Q3, as Q1 displays no sign of time variability during our observation (see below).

To reduce the prominence of noise in the trailed spectra, the 1D spectra were first smoothed by convolution with a gaussian function of sigma, $\sigma = 1.1$ Å (10 pixels). The spectra were then normalized by fitting a 4th order chebyshev function to the time-averaged data; the fit was checked to assure that it did not produce strong curvature in the vicinity of the spectral lines. All time-resolved spectra were divided by this continuum fit and then renormalized to ensure a continuum level of 1. The mean-subtracted spectra were prepared for plotting by subtracting the normalized time-averaged spectrum from each time-bin's normalized spectrum.

The Q2 trailed spectra are presented in figure 3. In N V a dark broad ($\sim 500\,\mathrm{km\,s^{-1}}$ across) feature shifts steadily to the red by about $500\,\mathrm{km\,s^{-1}}$. Examining the 1D spectra for the first and the second half of the observation separately, it becomes clear that this is due to a redwards shift in the entire absorption profile. This is too large to be accounted for by a radial velocity shift due to WD orbital motion, if the orbital parameters derived by Gilliland and Phillips (1982) are accepted.

A similarly broad dark feature is also seen in the Si IV and O V trailed spectra. However, compared to N V the shift
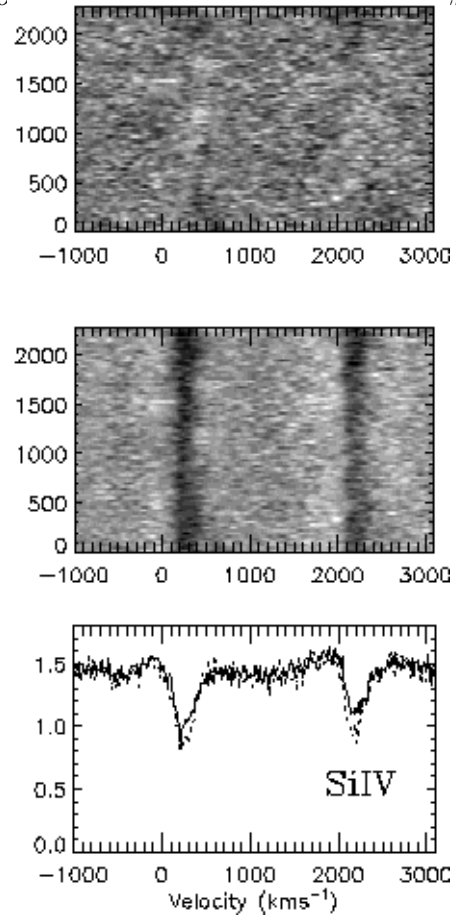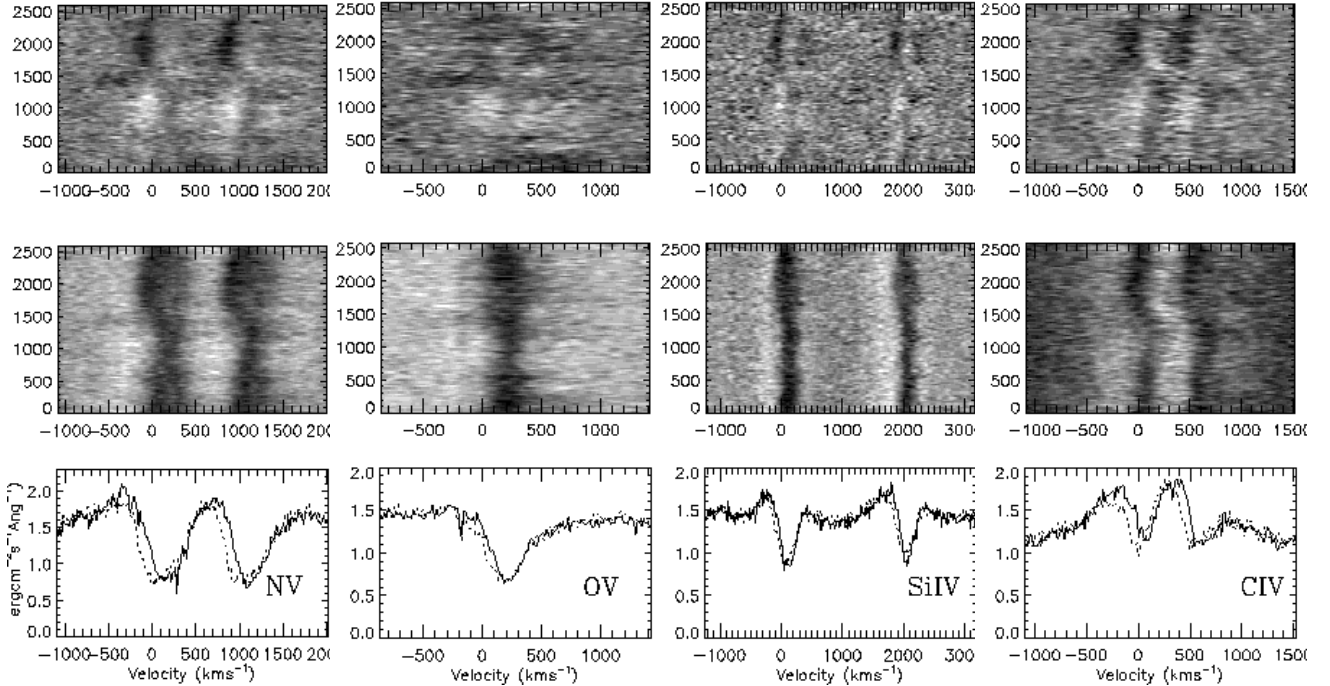

Figure 5. Greyscale difference spectrum of the Si IV λ 1398 line for Q1. The flux range is -0.22 to 0.24 (in mean-subtracted normalised flux units). Plotted beneath the stacked spectrum is the mean line profile for the first half of the observation (solid line) and the second half (dotted line).

is more abrupt at around the midpoint of the observation, fliping from blue to red in the space of less than 500 sec. Again, this feature represents a shift in the entire absorption profile from blue to red. Along with the redward shift there is also an alteration in the form of the O V and Si IV profiles, with the bluemost absorption wing becoming weaker and possibly even slightly emissive in Si IV. If more subtly, the C IV line appears to shift redwards in the same way as the N V line. Also, its broad redshifted emission component weakens slightly during the observation. No variation is detected in either the C III λ 1176 or He II λ 1640 lines.

In the Q3 trailed spectra (figure 4) there appears to be a velocity-shifting component to the line profiles: in the N V, Si IV and C IV lines a dark feature ($\sim 200\,\mathrm{km\,s^{-1}}$ wide) shifts gradually redwards by $\sim 200 - 300\,\mathrm{km\,s^{-1}}$ and then more sharply bluewards around the midpoint of the observation; this component then resumes its redwards shift, creating a 'sawtooth' pattern. As this variation occurs, the redward edge of these line profiles is very nearly stationary (see the lower panels in fig. 4). There is at most just a hint of the same behaviour in the O V line profile – the most obvious change is a slight weakening and narrowing of the absorption as a whole for about 300 sec centred on 1000 sec after the
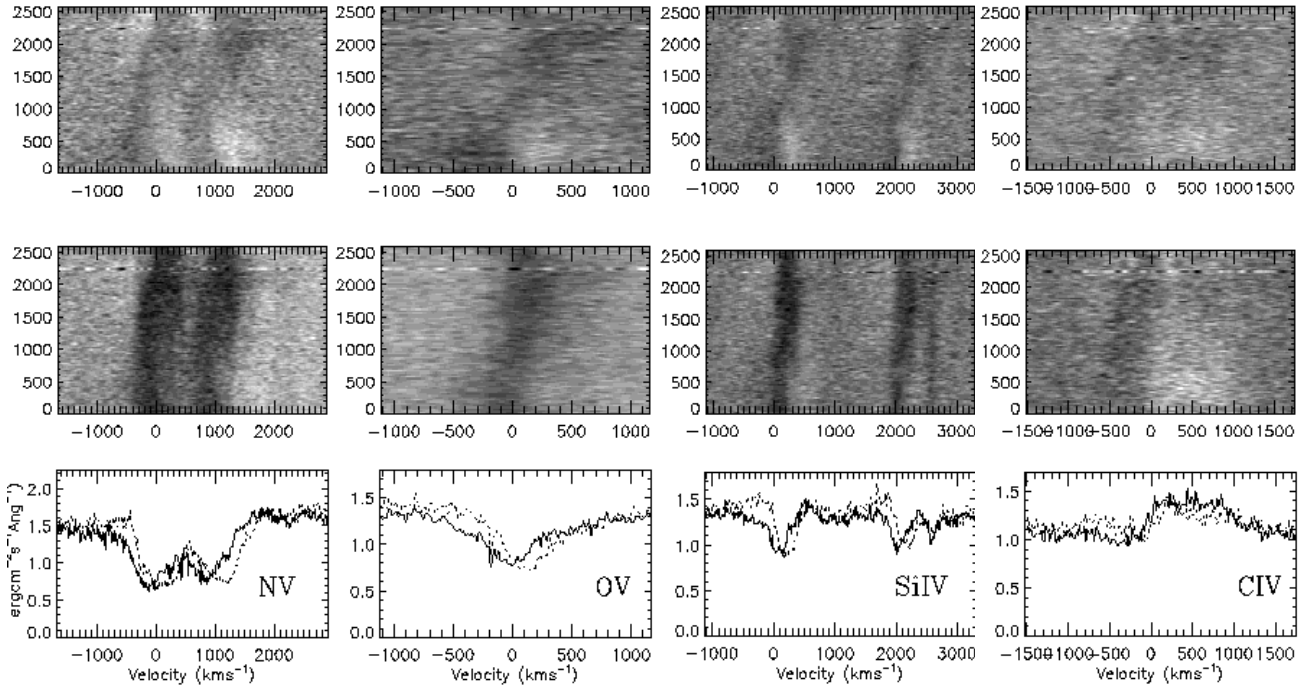
Figure 3. Mean-subtracted difference spectrum of (left to right, top to bottom) the N V λ 1240, O V λ 1371, Si IV λ 1398 and C IV λ 1549 lines for Q2. The flux range is as follows (in mean-subtracted normalised flux units): N V, -0.28 to 0.30; O V, -0.26 to 0.33; Si IV, -0.25 to 0.34; C IV, -0.44 to 0.49. Plotted beneath the stacked spectrum is the mean line profile for the first half of the observation (solid line) and th

Figure 4. Greyscale difference spectrum of (left to right, top to bottom) the N V λ 1240, O V λ 1371, Si IV λ 1398 and C IV λ 1549 lines for Q3. The flux range is as follows (in mean-subtracted normalised flux units): N V, -0.32 to 0.39; O V, -0.31 to 0.27; Si IV, -0.28 to 0.25; C IV, -0.40 to 0.46. Plotted beneath the stacked spectrum is the mean line profile for the first half of the observation (solid line) and the second half (dotted line).

start of the observation. Again, the C III and He II lines do not vary noticeably.

Q3 does reward with some sporadic, shorter timescale variablity. In the N V and O V trailed spectra there is a broadening of the absorption, appearing first in the red wing at around 1150 sec and then switching into the blue wing, finishing at about 1600 sec. In the C IV trailed spectrum, just the beginning of this change affecting the red wing of the line is detectable. There may also be a weaker event of the same kind at about 600 sec after the start, that again shows in the N V and O V profiles.

The variability seen in Q2 and Q3 is quite different. In Q2, there appears to be a shift in the gross line profiles accompanied by a small change in the steepness of the blue absorption edge. In Q3 the blue absorption edge shifts further to the blue, yielding an increase in the width of the line profile and only in this dataset is there any apparent variation on the ~ 100 sec timescale. In Q3, where line emission is generally more prominent, the variability persists as an attribute of the absorption line spectrum.

The lack of variabilty in observation Q1 is interesting as in the mean spectrum it bears a stronger resemblance to Q3 than the more variable Q2. Figure 5 shows the Q1 trailed data for Si IV λ 1398, the most variable of the transitions observed at this time. There is just a trace of the velocity-shifting component that is seen in the Q3 Si IV line. In the Q1 N V line profile there is a weak component of broad blueshifted absorption, signalling the presence of an outflow (see section 3). At the time of the Q3 observation there was no such evidence of outflow. It remains to be seen whether this anticorrelation is a persistent and hence significant effect.

In order to examine the data for continuum variability we plotted light-curves (figure 6) of flux summed over the 1450–1500 Å wavelength range, with time-binning of 20 s for each dataset. There is a similar contrast in the degree of continuum variability as that seen in the line profiles: Q1 exhibits almost no variability; Q2 shows some brightness change, dimming slightly towards the middle of the observation, and then recovering; finally, the lightcurve for Q3 has the most chaotic appearance of the three. The power spectrum was calculated for each of the three time series – in none was there evidence of any preferred periods of variation.

The detected UV light variation has an amplitude of around 10 per cent. This is consistent with optical estimates of photometric variability. Schild (1969) reported optical brightness fluctuations of up to 0.2 mag on a timescale of 90 sec. Similarly Gilliland and Phillips (1982) and Kern & Bookmyer (1986) presented photometric data showing variations of 0.1–0.2 mag on timescales of a few minutes.

5   COMPARISON WITH PREVIOUS *IUE* OBSERVATIONS

To set the characteristics of our high-quality *HST* UV spectra of QU Car in a broader context, we retrieved the 15 low-dispersion ($\Delta\lambda = 1.1$ Å) 1150–1975 Å spectra available from the *IUE* archive. These data are provided pre-calibrated in the NEWSIPS format and was extracted via the IUESIPS software run under IRAF.
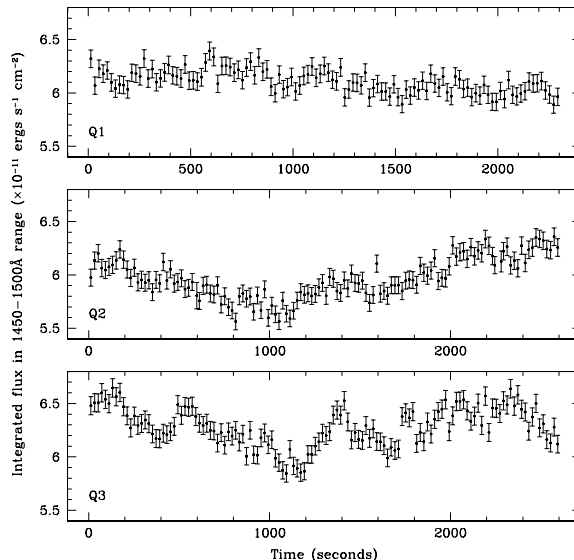

Figure 6. Light curve from each observation of QU Car. The flux is integrated over the wavelength range 1450–1500Å and the time-binning is 20 s.

The continuum flux level of our *HST* data is consistent with, but at the high end of that recorded in previous *IUE* observations in which it varies from a minimum of $\sim 1.38 \pm 0.09 \times 10^{-12}$ to maximum of $\sim 1.61 \pm 0.14 \times 10^{-12}$ erg s^{-1} cm^{-2} Å^{-1} (cf table 2). The *IUE* observations yield, on average, a slightly flatter dereddened continuum slope (-2.24 ± 0.13) than do the *HST* data (-2.34 ± 0.07).

As regards the spectral line behaviour, in contrast to the *IUE* data, the HST/STIS observations have caught QU Car at times when its C IV λ 1549 line presents with almost no blueshifted absorption. In all but three of the *IUE* spectra there is a significant blueshifted absorption component to the C IV line, extending to between -2000 and -2500 km s^{-1} of line centre. If this is taken to be the terminal velocity of an outflow, then this is relatively modest, compared to other CV, such as IX Vel and V3885 Sgr (Hartley et al. 2002) where the C IV line shows evidence of outflows up to at least 5000 km s^{-1}. In N V λ 1240, there is always a blueshifted absorption component. The proximity of the damped Lyα absorption may render this line less suitable, at the low resolution of the *IUE* low dispersion mode for a determination of typical maximum outflow speed. Nevertheless, measurement of the collected *IUE* data and the Q1 *HST* observation (figure 2) indicate that the maximum blueshift in the N V line generally matches that in C IV.

Figure 7 shows dataset Q1 downgraded to *IUE* resolution and overplotted on merged short-wavelength *IUE* data for 1981 December 7 (SWP15670, SWP15671), selected for being most similar to the *HST* sets, and merged data from 1991 June 26/27 (SWP51925-30), selected for showing much better developed wind signatures. We note that the He II emission is somewhat stronger in the *HST* sets than in all *IUE* observations. The O V λ 1371 line is present as a clear absorption feature in all UV spectra obtained to date. Putting all the available UV data together, there is no evidence that the equivalent width of the blueshifted absorp-
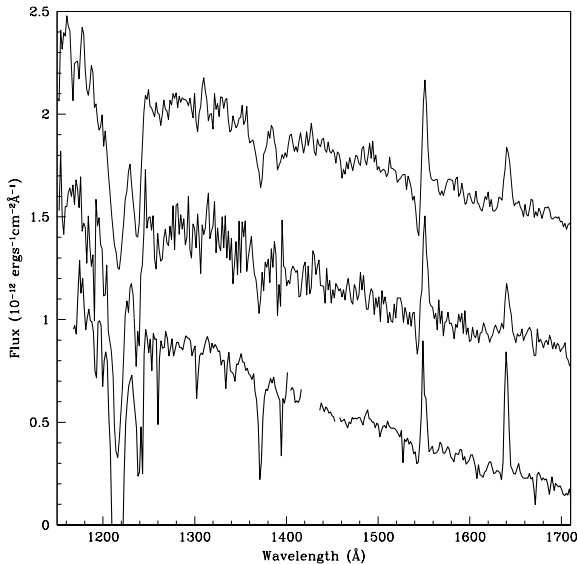
Figure 7. Two representative merged *IUE* spectra of QU Car compared to the Q1 *HST* spectrum downgraded to *IUE* resolution. The continuum level was approximately the same in all three observations. The *IUE* merged spectra SWP41925-30, obtained 26/27 June 1991, are plotted on the correct level, but for clarity, the *IUE* merged spectra SWP15670-1, obtained 7 Dec 1981, are offset upwards by 6×10^{-13} Å and the Q1 *HST* spectrum is offset downwards by 8×10^{-13} Å.

Figure 8. STIS spectrum of QU Car (dataset o5bi07010) compared to a GHRS spectrum of the dwarf nova SS Cyg in outburst (datasets Z3DV0104T and Z3DV0105T) and a STIS spectrum of the novalike variable IX Vel (dataset o5bi01010). All specta were downloaded via the MAST facility at the STScI.
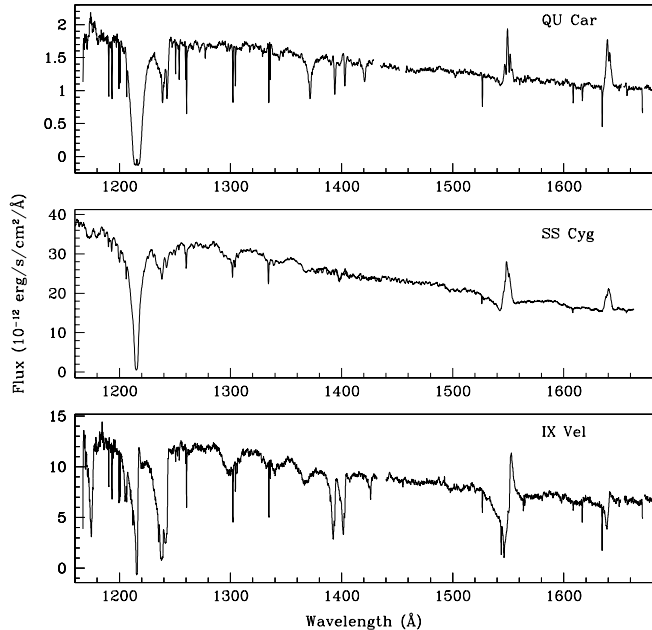
tion in the C IV and N V lines changes systematically with e.g. UV continuum brightness. Knigge et al. (1994) provide further discussion of variability in the *IUE* data.

Apart from the tendency for clearer wind signatures in the N V and C IV line profiles to appear in the *IUE* data (particularly those from the epoch studied by Knigge et al. 1994), there is strong consistency between these older observations and the new *HST* data. Encouraged by this, we can now turn to a summary discussion of what the higher-quality *HST* observations of QU Car have revealed to us about this highly-ionised compact binary.

6   DISCUSSION

In this paper we have presented high time- and high spectral-resolution UV spectra of QU Car obtained at three epochs. These data have pointed toward a higher than typical degree of ionization, and reveal a mix of fairly narrow, emission and absorption line features along with only modest evidence of mass loss.

Before considering the physical implications of the new spectroscopy, we review the constraints on the inclination of QU Car. Gilliland & Phillips proposed $i \lesssim 60°$ from the lack of orbital modulation in the binary's light curve and the relatively narrow optical emission features. The UV emission lines are not particularly broad either, generally fitting within approximately $\pm 1000 \, \mathrm{km \, s^{-1}}$. The simple fact that a number of UV spectral lines are firmly in absorption, and that broadened blueshifted absorption is detected from time to time, also reinforces the case for low inclination in that line emission is accepted as the general pattern for high-state

high inclination systems. We can venture a little further than this and note that the observed mix of emission and absorption lines argues persuasively against re-classifying QU Car as a magnetic system (see Warner 1995) – a step that might otherwise be contemplated on the grounds of the strong He II λ 1640 emission typifying this object.

We now compare the 1150–1660 Å spectrum of QU Car with those of more typical high-state non-magnetic CV in order to make the case that QU Car is extreme in terms of the apparent degree of ionization. We choose as our comparison objects SS Cyg near peak of outburst and IX Vel, for the reason that similarly high quality *HST* UV spectra have been obtained for them. IX Vel and SS Cyg are also non-eclipsing systems, like QU Car. The SS Cyg observations used (Z3DV0104T and Z3DV0105T) were obtained by one of us (KSL) and, to ensure the most up-to-date calibration, were retrieved from the MAST facility at STScI. The IX Vel observations were presented in Hartley et al (2002). The spectra of these three sources are shown together in figure 8. The three objects are placed in a sequence of increasing degree of ionization, with IX Vel the least-ionized, QU Car the most ionized and SS Cyg somewhere in between. This assessment is based largely on how the He II λ 1640 and O V λ 1371 line profiles compare with C IV λ 1549 – these signatures of high excitation are indeed relatively strongest in QU Car.

Anther point of contrast between QU Car and the other two systems concerns the broad absorption dips at $\sim$1300 Å and $\sim$1340 Å. These are presumably due to disc atmospheric blanketing. Wade & Hubeny (1998) show in their disc atmosphere models that these features would be expected to fade as the maximum disc temperature rises (see their fig-

ure 9). That this happens to at least the $\sim$1300 Å feature is consistent with the probable identification of much of the blend with modest-to-low ionization Si III/O I transitions. The pattern in figure 8 is that IX Vel presents with the highest equivalent width in these dips, SS Cyg is intermediate, whilst they are completely absent from QU Car. This trend operates in the same sense as the rise in relative prominence of the O V and He II lines.

Two final points of interest with regard to figure 8 are the larger number of interstellar lines in the spectrum of QU Car compared to either IX Vel or SS Cyg, and the appearance of both the C III λ1176 and C II λ1335 lines in emission in QU Car (albeit with a superposed absorption component in the former). The relatively rich interstellar line spectrum has to do with the greater distance to QU Car. This is estimated to be at least 500 pc (Gilliland & Phillips 1982), compared to 96 pc and 166 pc, from astrometric parallaxes, for IX Vel (*HIPPARCOS*) and SS Cyg (Harrison et al. 2001), respectively. The seeming predeliction for carbon line emission may be due to a carbon over-abundance in the emission line gas. Both the question of the distance to QU Car and the abundances issue are focused on in a separate study (Drew et al. 2002).

Although wind signatures are scarcely apparent in the QU Car spectrum shown in figure 8, the comparison with archive *IUE* data (section 5) showed that they have been more apparent at other epochs. However there is a clear point of contrast with objects like SS Cyg and IX Vel with regard to the maximum outflow velocities observed. In QU Car they are usually about 2000 km s^{-1}, whilst in both SS Cyg and IX Vel this is in the region of 4000 km s^{-1}. This higher figure is indeed typical of HnMCV (see e.g. Prinja & Rosen 1995). Very crudely, if it is assumed these speeds scale as the rotation speeds in the accretion disc where presumably the wind is launched, this factor of 2 difference may be viewed as implying a substantially larger launch radius in QU Car – perhaps up to a factor of 4 larger. Quantitatively this conclusion is somewhat dependent on both the binary inclination and accretor mass – qualitatively it will be hard to avoid. Its implication, like the impression of relatively high ionization, is a higher than typical mass accretion rate.

In the above we have assumed that the UV continuum emission in QU Car is dominated by disc accretion. This seems uncontroversial given the similarity between the slope of its dereddened energy distribution and that of indisputably accretion-dominated HnMCV (see section 3). It is likely that all absorption features, including those seen superposed on the C III, C IV and He II emission profiles, form in the disc atmosphere. This view is supported by the way in which the pattern of variability seen in N V and Si IV absorption during the Q3 observation is also apparent in the C IV absorption component. The less variable He II absorption component can be viewed as mimicking the less variable O V profile.

We now consider the likely origin of the line emission. Figure 9 shows the emission, from the three ionization stages of carbon present in the spectrum, plotted on a common velocity scale. The C II line is clearly the narrowest with a HWZI of order 600 km s^{-1}. The HWZIs in the C III and C IV lines are not so easy to tell apart. On fitting a single gaussian through the line wings we find that the FWHM, respectively for these two lines, is $\sim$950 km s^{-1} and $\sim$1100 km s^{-1}. These
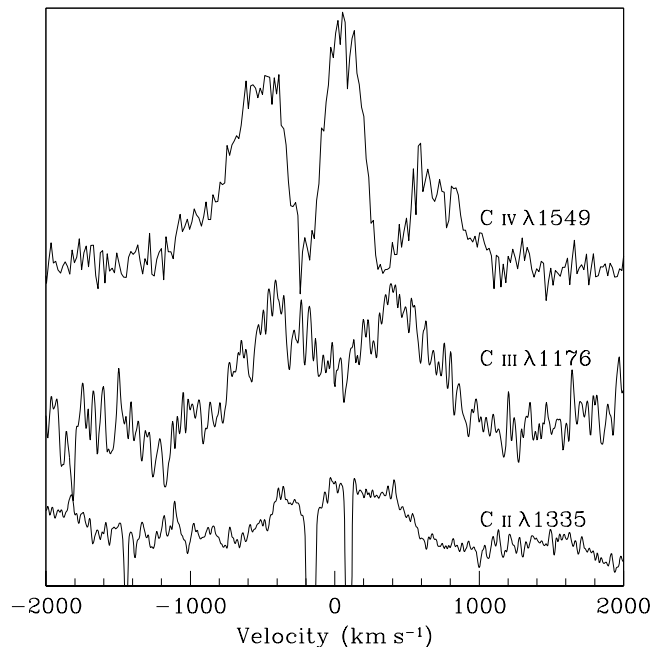
Figure 9. Three ionisation stages of carbon present in the UV spectrum: C III λ1176, C II λ1335 and C IV λ1549, plotted on the same velocity scale. The C II and C III lines are taken from a mean of the three STIS spectra to improve the S/N ration, whereas the C IV line is taken from I3. The narrow absorptions superposed on the C II line are interstellar lines formed in the same transition.

figures translate to HWZIs of $\sim$1200 and $\sim$1400 km s^{-1}. We do not correct for intrinsic multiplet splitting because the magnitude of the correction depends on the unknown flux ratios among the multiplet components. Fortunately these splittings are not so large that correction for them would alter the basic finding – namely, that broader emission is associated with higher ionization. The near equality of the C III and C IV emission widths probably indicates that the excited C III line contains a substantial contribution from recombination.

To see all three carbon ion stages simultaneously, with this pattern of velocity widths probably points to an origin in a disc 'chromosphere'. This might be created by irradiation from the EUV-bright inner disc and accreting object. Emission produced by an outflow from the accretor or the innermost disc is rendered less likely by the modest ionization of the C II and C III lines (with the emissive flux in the C III line only a little less than that in C IV). Since the emission component in each of the C III, C IV and He II lines is broader than the superposed absorption, we would have to refer to a specific kinematic model for the system to position the emission line region relative to the absorption line region. In the absence of this, we cannot distinguish whether the line emission is optically thin and overlies the source of line absorption, or whether it comes from a different part of the disc.

The emergent picture of QU Car is then that it is relatively highly-ionized compared to the more typical properties of HnMCV. The narrowness of the UV spectral lines observed may have to do with their production at larger

disc radii than usual. Of course we cannot yet rule out the possibility that QU Car might be oriented nearly pole on.

We have to leave as an unsolved mystery the origin of the short-term variability within the spectral line profiles (section 4) that has been revealed thanks to the HST/STIS TIME-TAG mode of data-taking. Since this variability is not present at all epochs and indeed presents with different properties on the two occasions we have noticed it, it is unlikely to be connected to anything as fundamental as the binary orbit. Our third set of data hints at a repetition timescale of around an hour if, that is, the detected absorption profile disturbances do in fact repeat. To progress any further, another more intensive campaign of spectroscopic observation would be required.

Lastly, we have not yet been able to begin to find an explanation for the remarkable inverse P Cygni character of, most notably, the N V λ 1240 and Si IV λ 1397 line profiles detected in our third dataset. It is already clear that QU Car is a remarkable binary that has been overlooked for too long. In a separate study focusing on exploitation of the UV interstellar line data and new optical spectroscopy (Drew et al. 2002), we show that this binary may in fact be closely related to the supersoft sources and then present evidence of carbon over-abundance. It is to be hoped that this re-evaluation of the status of QU Car and the presentation here, of its striking UV spectroscopic properties, will significantly broaden our perception of the ways the Universe finds to configure such high-state compact binaries.

REFERENCES

Downes R. A., Webbink R. F., Shara M. M., Ritter H., Kolb U., Duerbeck H. W., 2001, PASP, 113, 764 ,

Drew J. E., Hartley L. E., Long K. S., 2002, MNRAS, to be submitted

Gilliand R. L., Phillips M. M., 1982, ApJ, 261, 617

Harrison T E., McNamara B J., Szkody P, McArthur B. E., Benedict G. F., Klemola A. R., Gilliland R. L., 1999, ApJ, 515, 93

Hartley L. E., Drew J. E., Long K. S., Knigge C., Proga D., 2002, MNRAS, 332, 127

Kern J. R., Bookmyer B. B., 1986, PAS, 98, 1336

Knigge C., Drew J. E., Hoare M. G., La Dous C., 1994, MNRAS, 269, 891

Prinja R. K., Rosen R.,1995, MNRAS, 273, 461

Proga D., Stone J., Drew J. E., 1998, MNRAS, 295, 595

Ritter H., Kolb U., A&AS, 129, 83

Schild R. E., 1969, ApJ, 157, 709

Verbunt, F., 1987, AASS, 71, 339

Warner B., 1995, Cataclysmic Variable Stars, 1st edn. Cambridge Univ. Press, Cambridge